

We are IntechOpen, the world's leading publisher of Open Access books Built by scientists, for scientists

6,900

Open access books available

186,000

International authors and editors

200M

Downloads

Our authors are among the

154

Countries delivered to

TOP 1%

most cited scientists

12.2%

Contributors from top 500 universities



WEB OF SCIENCE™

Selection of our books indexed in the Book Citation Index
in Web of Science™ Core Collection (BKCI)

Interested in publishing with us?
Contact book.department@intechopen.com

Numbers displayed above are based on latest data collected.
For more information visit www.intechopen.com



Aligned Growth of Single-Walled and Double-Walled Carbon Nanotube Films by Control of Catalyst Preparation

Mineo Hiramatsu¹ and Masaru Hori²

¹*Meijo University,*

²*Nagoya University
Japan*

1. Introduction

Carbon nanotubes (CNTs) have attracted significant attention for various potential applications, such as electron field emitter arrays and multi-level interconnections of ultra-large scale next-generation integrated circuits (IC). Many of the proposed applications of CNTs require aligned nanotubes grown on a substrate. Among the various methods used for growing CNTs, plasma-enhanced chemical vapor deposition (CVD) has attracted considerable attention for industrial applications due to its feasibility and potential for large-area production with reasonable growth rates at relatively low temperatures.

For the growth of CNTs on a silicon (Si) substrate or other substrates by CVD, a catalyst metal, such as iron (Fe) or cobalt (Co) is indispensable. The diameters of CNTs almost correspond to the size of the metal catalyst islands or particles on the heated substrate immediately before the supply of a carbon source gas, such as methane (CH₄), ethylene (C₂H₄), and acetylene (C₂H₂). In order to obtain single-walled carbon nanotubes (SWNTs) or double-walled carbon nanotubes (DWNTs) by the CVD method, it is important to control the size of the catalytic particles to approximately several nanometers or less. When using a Si substrate, the formation of metal-silicide as a result of the preheating treatment will complicate the synthesis process. Previously, buffer layers using Al, Ti or SiO₂ have been used in order to prevent the formation of metal-silicide (Lee et al., 2003; Kim et al., 2001; Hong et al., 2001). However, it is still difficult to simultaneously control both the catalyst particles' size and the density on the substrate surface. Therefore, control over the preparation of catalytic nanoparticles on the substrate is essential to be able to control the diameters of the nanotubes and to obtain the optimum potential of the CNTs.

In this chapter, growth of aligned CNT films using microwave plasma-enhanced CVD is described, with a particular emphasis on the pretreatment of substrate with catalytic metal nanoparticles. By preparing the Co nanoparticles in a controlled manner, aligned SWNT and DWNT films were fabricated on the Si substrate. Furthermore, area-selective growth of vertical CNTs to form organized SWNT and DWNT microstructures was demonstrated.

2. Catalyst particle preparation

When using plasma-enhanced CVD to synthesize CNTs on a substrate, conventionally a catalytic metal thin film is formed on the substrate by sputtering or evaporation methods,

and the substrate is typically preheated in order to form catalytic nano-islands in the range of 10–100 nm, prior to the CNT growth. The sizes of the catalyst islands depend on the initial thickness of the catalytic metal thin film. As shown in Fig. 1, thicker catalyst film yields relatively larger catalyst islands, and sometimes multiple CNTs are grown from one catalyst nano-island. On the other hand, thinner film results in the formation of smaller catalyst islands with less density. The control of the size and density of catalyst nanoparticles on the substrate is desirable.

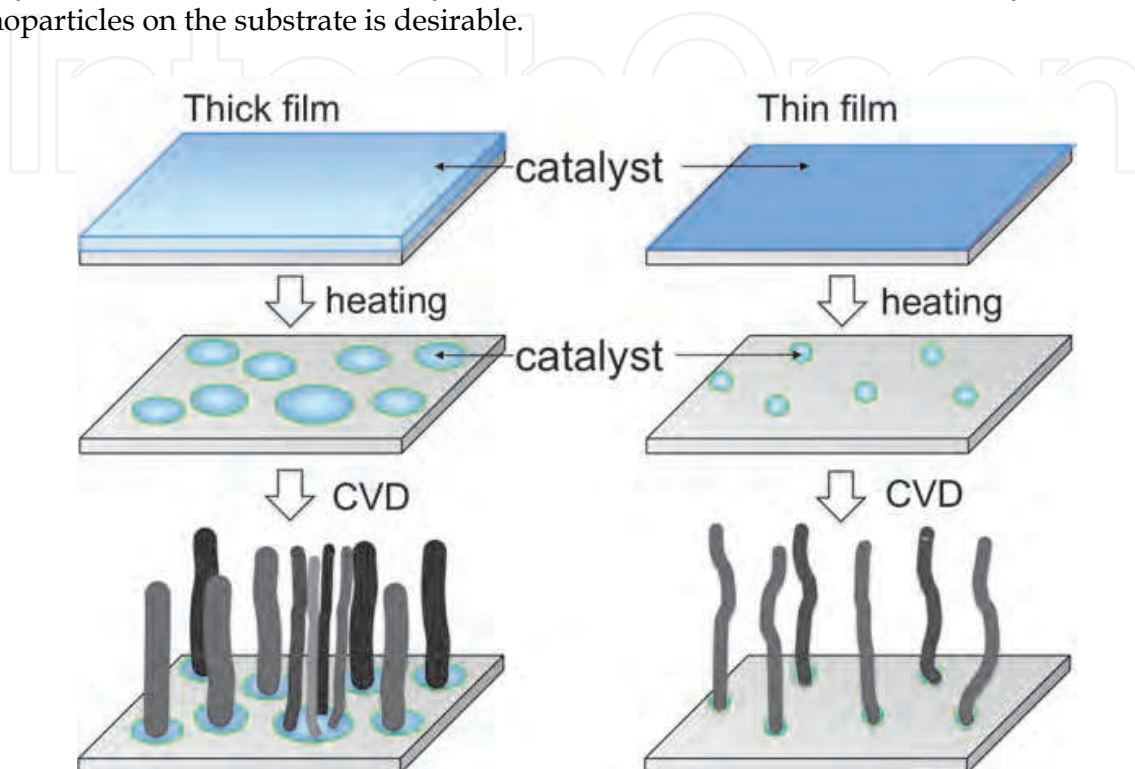


Fig. 1. Schematic of conventional procedure for preparing catalyst nanoparticles or nanoislands and subsequent CVD growth

As a method of controlling the size of catalyst metal islands or particles, zeolite has been used as a support for the catalytic particles. In this method, the size of the catalytic particles is uniformly controlled using the pores of the zeolite as a template, and SWNTs or DWNTs with relatively uniform diameters can be grown (Sugai et al., 2003, 2004). The growth of vertically aligned SWNTs was demonstrated using a catalytic CVD method on a quartz substrate with mono-dispersed Co–Mo catalysts, with 1–2 nm particle size, prepared by a dip-coating method (Murakami et al., 2004). The low temperature growth of aligned SWNTs was attained using a sandwich-like nano-layered structure of Al_2O_3 (0.7 nm)/Fe (0.5 nm)/ Al_2O_3 (5–70 nm) for the preparation of catalytic Fe nanoparticles on a Si substrate (Zhong et al., 2004).

Laser ablation of a metallic target to obtain catalytic particles is effective for preparing high-density catalytic nanoparticles, and the laser ablation technique for catalyst preparation enables the formation of aligned nanotube films with nanotubes diameters of 5 to 10 nm (Hiramatsu et al., 2005). Figure 2 shows a schematic of laser ablation system used for the preparation of catalyst nanoparticles. In this case, KrF excimer laser (wavelength: 248 nm) is used for the ablation of Co target. The excimer laser ablation yields Co nanoparticles with a size of 5–10 nm.

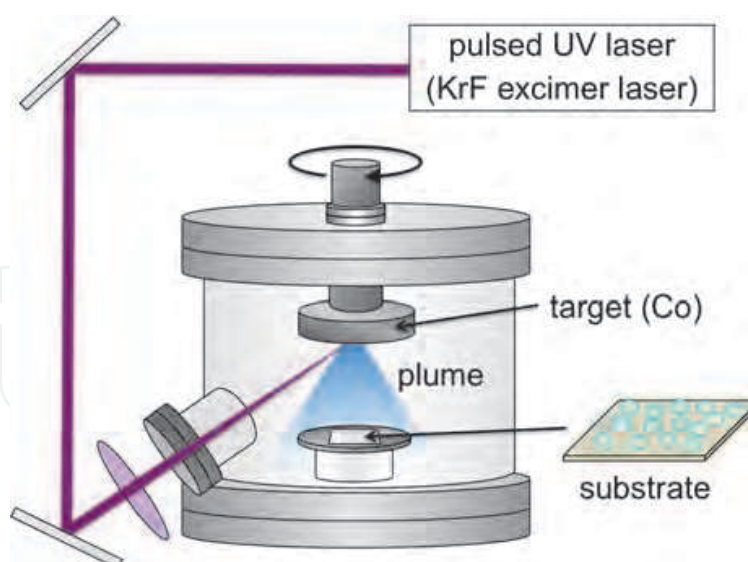


Fig. 2. Schematic of laser ablation system used for the preparation of catalyst nanoparticles

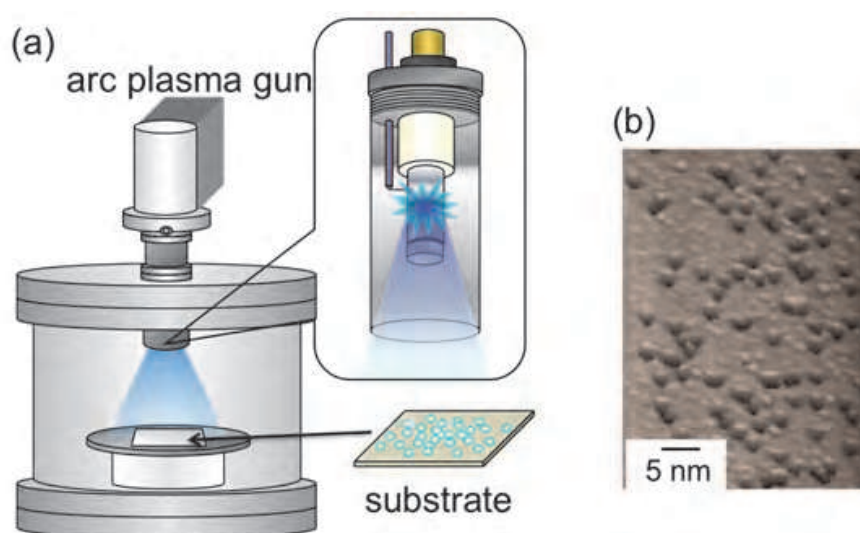


Fig. 3. (a) Schematic of pulsed arc deposition system used for the preparation of catalyst nanoparticles. (b) AFM image of Co-catalyzed Si substrate prepared using pulsed arc discharge. The number of pulses of the arc discharge was 10 shots. (Hiramatsu et al., 2007b) - reproduced with permission from Institute of Pure and Applied Physics

On the other hand, pulsed arc deposition is effective for the preparation of catalyst nanoparticles with a size of 1–2 nm. Figure 3(a) shows a schematic of nanoparticle preparation system using pulsed arc plasma deposition (Arc plasma gun, ULVAC, Inc.) (Agawa et al., 2003; Yamamoto et al., 1998). As a preliminary experiment, Co nanoparticles were directly formed on the Si substrate by pulsed arc discharge. Figure 3(b) shows an atomic force microscopy (AFM) image of the Co-catalyzed Si substrate prepared by pulsed arc discharge with a Co electrode. The number of arc discharge pulses was 10 shots in this case. The cumulative particle density of Co nanoparticles on the substrate was estimated to be $8 \times 10^{11} \text{ cm}^{-2}$ after 10 shots of pulsed arc discharges with the Co electrode. It was found that the pulsed arc plasma deposition yielded Co nanoparticles smaller than those formed

by laser ablation method, according to the AFM observations shown in Fig. 3(b). The size of Co nanoparticles estimated from the height in AFM is approximately 1–2 nm, which would be suitable for the growth of SWNTs or DWNTs. Actually, in the case of CNT growth on the Si substrate, the formation of metal-silicide as a result of substrate heating process complicates the synthesis process; silicide cannot act as catalyst for CNT growth. Therefore, in our case, Ti or TiN is used as a buffer layer in order to prevent the formation of Co silicide during the rise in temperature, just before introducing carbon source gas into the reaction chamber.

3. CNT growth system using microwave plasma-enhanced CVD

Microwave plasma is one of high-density plasmas and is suitable for decomposing H_2 molecules to generate H atoms effectively. Figure 4 shows a microwave plasma-enhanced chemical vapor deposition (CVD) system, which has been called ASTeX (Applied Science and Technology, Inc.) type. This system has been extensively used for the growth of diamond films. The ASTeX-type reactor consists of a cylindrical stainless steel chamber. The microwave (2.45 GHz) is coupled from the rectangular waveguide into the cavity via an axial antenna. A discharge called a “plasma ball” is generated above the substrate. The plasma ball provides the substrate heating. The CVD process would be operated at pressures of a few tens of Torr (10^3 – 10^4 Pa), and the reactor pressure and microwave power cannot be varied completely independently. At too high pressure or low microwave power, plasma cannot be sustained. On the other hand, if the microwave power is too high for a given pressure, the plasma becomes unstable and tends to jump to the quartz (fused silica) window, occasionally resulting in the destruction of the window by the heat.

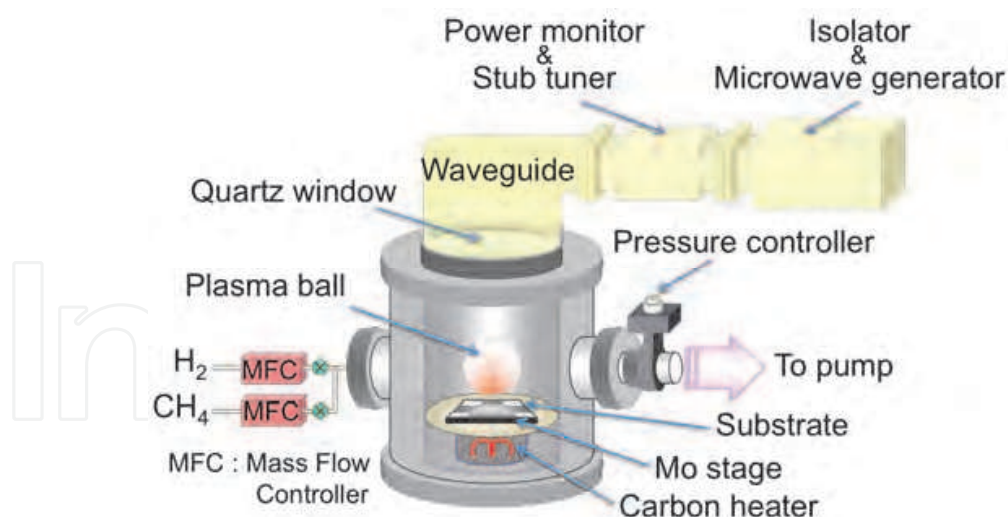


Fig. 4. Schematic of microwave plasma-enhanced CVD system used for CNT growth

In the case of diamond growth, deposition is carried out in a mixture of CH_4 or C_2H_2 and H_2 at substrate temperatures of 700–800 °C. Typical H_2/CH_4 flow rate ratio is about 100. The high H_2/CH_4 flow rate ratio for diamond growth is essential to remove unwanted non-diamond phase. In the case of the synthesis of CNTs, on the other hand, deposition process is carried out at a low H_2/CH_4 flow rate ratio of 1–4. In the present study, CNT films were grown using conventional microwave plasma-enhanced CVD with a 2.45 GHz, 1.5 kW

microwave generator. The reactor consists of a cylindrical stainless steel chamber with an inner diameter of 11 cm, and a molybdenum (Mo) substrate stage with a graphite heater that allows for control of the substrate temperature, independent of the microwave input power. The flow rates of CH₄ and H₂ were 50 and 70 sccm, respectively. The microwave power and total pressure were maintained at 900 W and 70 Torr, respectively. Substrates used for the growth experiments were Si (100). Scanning electron microscopy (SEM) and transmission electron microscopy (TEM) were used to evaluate the morphology of the grown CNTs. Raman spectra for the CNTs were obtained using the 514.5 nm line of an Ar laser and the 632.8 nm line of an He-Ne laser.

4. CNT growth experiments

4.1 CNT growth from Co nanoparticles prepared using pulsed laser ablation

Growth experiments were carried out using microwave plasma-enhanced CVD on the Co-catalyzed Si substrate at 700 °C. Co nanoparticles of 5–10 nm size as catalyst were prepared by KrF excimer laser (248 nm) ablation using a 99.998% Co target in vacuum at a pressure of 10⁻⁴ Torr at room temperature. The energy density of the excimer laser beam at the target surface was maintained at 5 J/cm² at a repetition rate of 20 Hz. The distance between the Co target and substrate was approximately 10 cm. The density of Co nanoparticles on the substrate was controlled by varying the ablation period from 60 to 300 min. Furthermore, a TiN thin layer with a thickness of 20 nm was prepared on the Si substrate as a buffer layer to prevent the formation of Co silicide. No heat pretreatment for the catalyst was performed prior to the CNT growth.

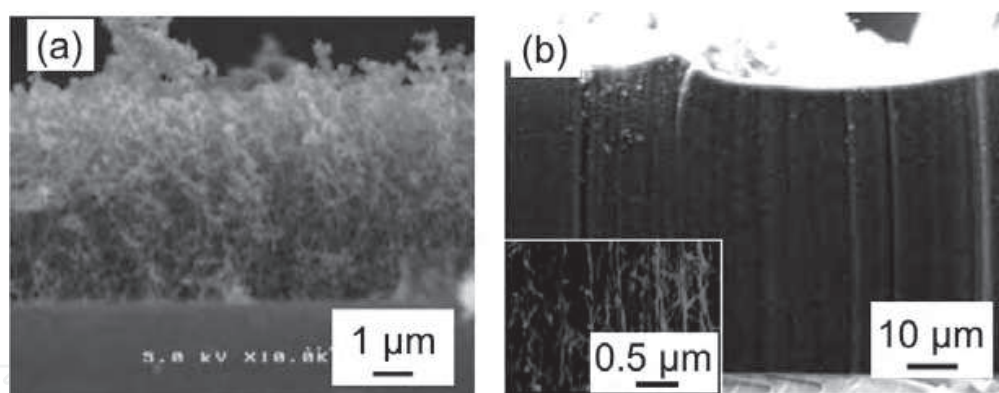


Fig. 5. (a) Cross-sectional SEM image of CNTs with random orientation grown from Co nanoparticles without buffer layer. (b) Cross-sectional SEM image of dense CNT film grown from Co nanoparticles with TiN buffer layer. Inset shows magnified SEM image of dense CNT film. (Hiramatsu et al., 2005) - reproduced with permission from Institute of Pure and Applied Physics

Figure 5(a) shows a cross-sectional SEM image of CNTs grown for 5 min on the Co-catalyzed Si substrate without a buffer layer. As shown in Fig. 5(a), without buffer layer, randomly oriented, curly CNTs with a low density were grown, but the alignment of CNTs was not obtained. Figure 5(b) shows a cross-sectional SEM image of the CNT film grown from Co nanoparticles with TiN buffer layer. In this case, Co nanoparticles were deposited for 180 min, which was nearly optimum condition for dense nucleation. Vertically aligned, dense CNTs were grown, as shown in Fig. 5(b). A magnified SEM image of the dense

nanotube film is shown in the inset of Fig. 5(b), indicating that the aligned nanotube forests were composed of nanotube bundles supporting one another. The presence of a TiN buffer layer was found to be effective for CNT growth on a Si substrate.

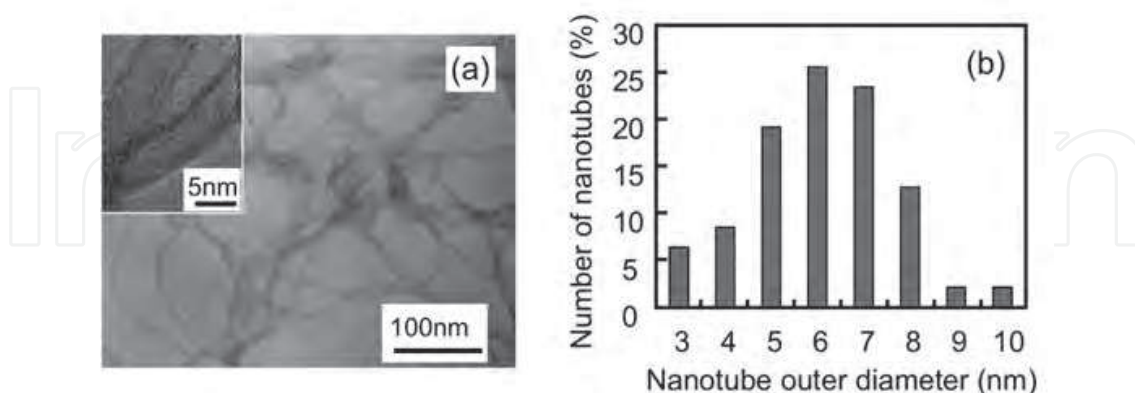


Fig. 6. (a) TEM image of CNTs. (b) Distribution histogram of nanotube outer diameters deduced from TEM observation. (Hiramatsu et al., 2005a) - reproduced with permission from Institute of Pure and Applied Physics

Figure 6(a) shows a typical TEM image of CNTs that were scraped away from the substrate surface and were ultrasonicated in methanol. Note that no Co particles were observed at the nanotube tips with TEM. As shown in the inset of Fig. 6(a), a TEM image reveals the multiwalled structure of the CNTs, containing a clear inner channel with an inner diameter of approximately 4 nm, surrounded by 2 – 5 concentric walls. Figure 6(b) shows a distribution histogram of nanotube outer diameters. CNTs grown using laser-ablated Co nanoparticles had small average diameters and a relatively narrow diameter distribution centered at approximately 6 nm. It was reported that nanotube growth rate was inversely proportional to nanotube diameter (Bower et al., 2000). Namely, the smaller diameter nanotubes would grow at a faster rate in terms of height. In this case, the size of Co islands formed by laser ablation was relatively small and remained unchanged with increasing substrate temperature just before CNT growth, due to the existence of a TiN buffer layer that prevented the formation of Co silicide. Therefore, these Co nanoparticles play an important role as a template for CNT growth, resulting in the determination of nanotube diameters as small as 6 nm and consequently, a high-rate growth of CNTs could be attained. The most significant difference from previous reports is that the catalyst was prepared originally in the form of nanoparticles in this case. Therefore, a nanotube diameter as small as approximately 6 nm was determined by the size of Co particles formed on the TiN buffer layer by laser ablation, resulting in the rapid growth of CNTs at 300 nm/s.

4.2 DWNT growth from Co catalysed Si prepared using pulsed arc discharge

As mentioned before, the pulsed arc plasma discharge can yield metal nanoparticles with a size of 1–2 nm, as shown in Fig. 3(b). Meanwhile, it has proven that the presence of a TiN buffer layer is effective for CNT growth on a Si substrate. Accordingly, in order to prepare smaller catalyst nanoparticles for growing CNTs with small diameters, pulsed arc discharge plasma was utilized to prepare Co nanoparticles on the Si substrate with TiN buffer layer. Substrate treatment was performed as follows (Fig. 7). First, a thin TiN layer with thickness of 20 nm was prepared on the Si substrate. The TiN thin layer plays an important role as a

buffer layer to prevent the formation of Co silicide during the heating process, just prior to the introduction of CH_4 gas into the reaction chamber. Co particles were then deposited on the TiN buffer layer using pulsed arc plasma deposition (Arc plasma gun, ULVAC, Inc.) in vacuum, at a pressure of 10^{-4} Torr at room temperature. The arc plasma gun was operated intermittently in a pulsed operation. No heat pre-treatment was performed for the catalyst prior to the CNT growth process. The density of Co nanoparticles on the substrate was controlled by varying the number of pulses in the range from 50 to 250 shots, corresponding to the particle number density of 4×10^{12} to $2 \times 10^{13} \text{ cm}^{-2}$ on the surface. A mixture of CH_4 and H_2 was used as the source gas. The flow rates of CH_4 and H_2 were 50 and 70 sccm, respectively. The microwave power and total pressure were maintained at 900 W and 70 Torr, respectively. CNTs were grown on the Co-catalyzed Si substrates in the presence of a TiN buffer layer at a substrate temperature of 700°C .

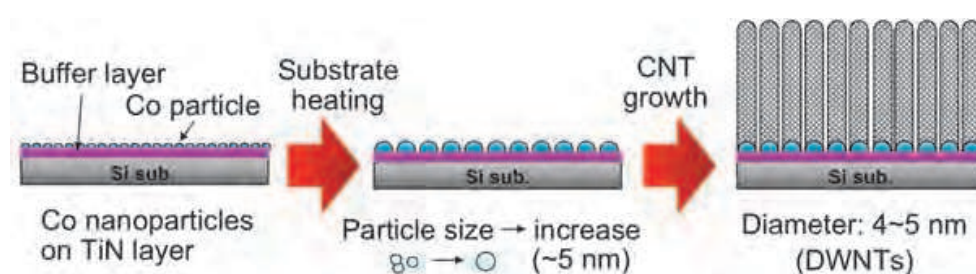


Fig. 7. Schematic of catalyst preparation for growing CNTs with small diameters (DWNTs)

Figure 8 shows a SEM image of Co-catalyzed Si substrate just before introducing CH_4 at substrate temperature of 700°C . Co particles were prepared using pulsed arc plasma deposition with 250 pulses, corresponding to the cumulative particle number density of approximately $2 \times 10^{13} \text{ cm}^{-2}$ on the surface. It was found that Co nanoparticles with size of 4–5 nm were formed on the TiN buffer layer. The pulsed arc plasma deposition using the arc plasma gun yielded Co nanoparticles of about 1–2 nm in size, according to AFM observations of the Co-catalyzed substrate without the TiN buffer layer as shown in Fig. 3(b). In our system, it takes about 10 min to increase the substrate temperature from room temperature to 700°C . During this period, the overlapped or closely adjacent particles would aggregate, presumably resulting in the formation of Co nanoislands of about 3–5 nm in size, which would be suitable for the nucleation of double-walled CNTs.

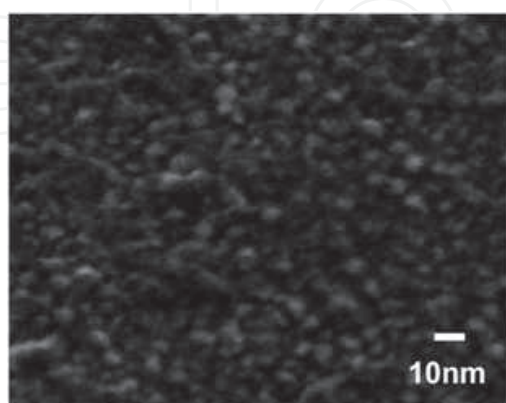


Fig. 8. SEM image of Co-catalyzed Si substrate just before introducing CH_4 at substrate temperature of 700°C . Co particles were prepared using pulsed arc plasma deposition with 250 pulses. The cumulative Co particle number density was $2 \times 10^{13} \text{ cm}^{-2}$ on the surface.

Figures 9(a) and 9(b) show typical cross-sectional and top-view SEM images of the CNT film, respectively. Figures 9(c) and 9(d) show close-up images of the cleaved CNT film. From the morphology observed in Fig. 9(d), it can be seen that individual CNT bundles grew almost vertically via a self-supporting mechanism, due to the extremely high density of the CNTs.

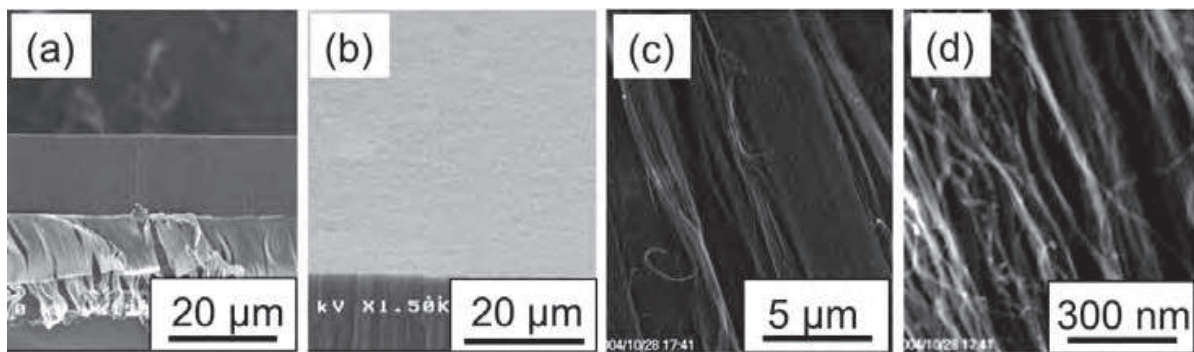


Fig. 9. SEM micrographs of CNT films grown on a Co-catalyzed Si substrate with a TiN buffer layer. The Co particles were prepared using pulsed arc plasma deposition with 250 pulses. (a) Cross-sectional SEM image of the dense CNT film. (b) SEM image showing the surface of the CNT film, (c)(d) Close-up images of cleaved CNT film showing aligned growth of the nanotubes. (Hiramatsu et al., 2005b) - reproduced with permission from Institute of Pure and Applied Physics

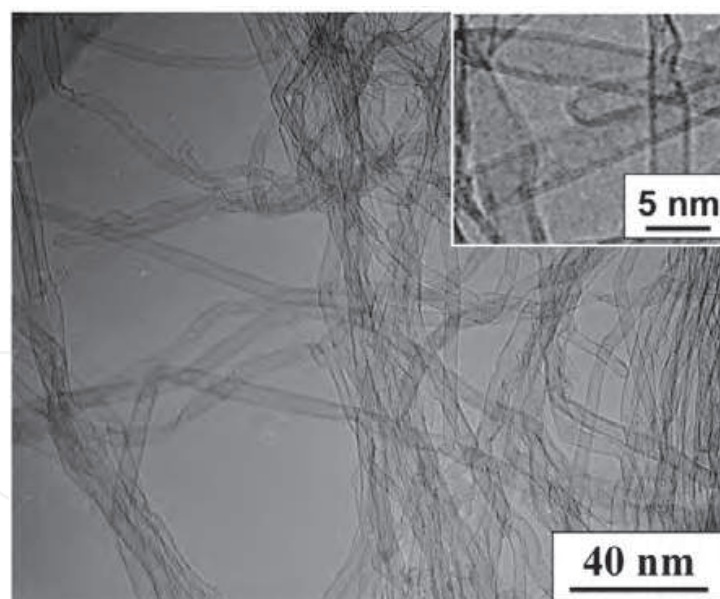


Fig. 10. TEM image of CNTs scraped from the substrate. The CNTs were grown on the Co-catalyzed Si substrates at a substrate temperature of 700 °C. The inset shows a magnified TEM image of typical CNTs. (Hiramatsu et al., 2005b) - reproduced with permission from Institute of Pure and Applied Physics

Figure 10 shows a low-magnification TEM image of typical CNTs. Co nanoarticles were prepared using pulsed arc plasma deposition with 50 pulses. The TEM specimen in Fig. 10 was scraped away from the substrate and was ultrasonicated in methanol. The CNTs are

hollow and have a small average diameter of approximately 4.5 nm. Note that no Co particles were observed at the nanotube tips in the TEM micrographs. As shown in the inset of Fig. 10, a magnified TEM image reveals that most of CNTs have a double-walled structure, with a clear inner channel of approximately 4 nm inner diameter. The percentages of single-, double- and triple-walled CNTs were estimated to be 5%, 80%, 15%, respectively. A growth rate curve for the CNT film was obtained by measuring the thickness of the CNT films for different growth periods, according to the observation of cross-sectional SEM images of CNT films. Figure 11 shows the average thickness of the aligned CNT film as a function of the growth period. As shown in Fig. 11, the thickness of the CNT film increased linearly up to 10 min and the CNTs grew at an extremely high rate of 600 nm/s during the first 10 min. Dense DWNT films with a thickness over 500 μm were obtained after 20 min.

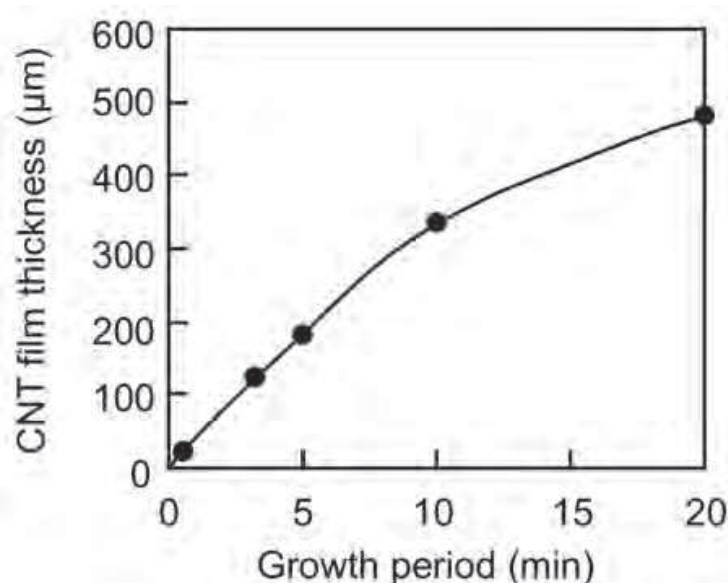


Fig. 11. Average thickness of aligned CNT films as a function of growth period. Co particles were prepared using pulsed arc plasma deposition with 250 pulses. The cumulative Co particle number density was $2 \times 10^{13} \text{ cm}^{-2}$ on the surface. (Hiramatsu et al., 2005b) - reproduced with permission from Institute of Pure and Applied Physics

Figure 12 shows distributions of the nanotube outer diameters grown from Co nanoparticles of different number densities. Co particles were prepared using pulsed arc plasma deposition with 50 (closed circles) and 250 (open circles) pulses, corresponding to the Co particle number densities of 4×10^{12} and $2 \times 10^{13} \text{ cm}^{-2}$ on the surface, respectively. In the case of growth on Co-catalyzed Si substrates with cumulative Co nanoparticle density of $2 \times 10^{13} \text{ cm}^{-2}$ (250 pulses), the CNTs had small average diameters of the nanotubes and a narrow diameter distribution centered around 4.5 nm. On one hand, in the case of the CNTs grown with Co nanoparticle density of $4 \times 10^{12} \text{ cm}^{-2}$ (50 pulses), average outer diameter of CNTs decreased to 3.5–4 nm. The most significant difference from previous reports is that the catalyst was prepared originally in the form of nanoparticles in our study. It has been reported that the nanotube growth rate is inversely proportional to the nanotube diameter (Bower et al., 2000). Namely, the smaller diameter nanotubes would grow at a faster rate in terms of height. In this study, the sizes of the Co particles formed by pulsed arc deposition were relatively small. The resultant Co nanoislands thus clearly play an important role as a

template for CNT growth, yielding nanotube diameters as small as 4–5 nm in the case of 250 pulses, for example, and consequently, a fast rate of growth could be attained for the CNTs. The density of nanotubes was roughly estimated to be 10^{12} cm^{-2} for the CNTs grown on a Co-catalyzed Si substrate, with a cumulative Co nanoparticle density of $2 \times 10^{13} \text{ cm}^{-2}$ (250 pulses).

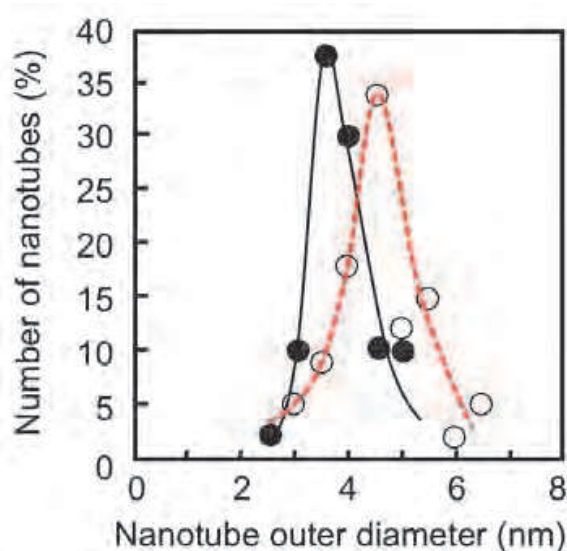


Fig. 12. Distributions of nanotube outer diameters deduced from TEM observations. Co particles were prepared using pulsed arc plasma deposition with 50 (closed circles) and 250 (open circles) pulses, corresponding to the cumulative Co particle number density of 4×10^{12} and $2 \times 10^{13} \text{ cm}^{-2}$ on the surface, respectively. (Hiramatsu et al., 2005b)

Figure 13 shows a variation of thickness of DWNT films grown for 3 min and corresponding growth rate as a function of number of pulses of the pulsed arc discharge plasma for the preparation of Co nanoparticles (or estimated cumulative Co nanoparticle number density on the TiN buffer layer). As the cumulative Co particle number density on the substrate increased, the growth rate of the DWNT film increased up to 600 nm/s, as shown in Fig. 13. Too many Co particles on the substrate lead to the increase of the size of Co nanoislands formed during the heating process, resulting in the growth of multiwalled (≥ 3 layers) CNTs with lower growth rate. On the other hand, as the cumulative Co nanoparticle number density on the substrate decreased, average diameter of grown DWNTs decreased slightly as can be seen from Fig. 12, and the growth rate of DWNT films decreased. The reduction of growth rate is attributed to the increase of free space to grow for individual tubes, due to the decrease in the density of Co nanoislands formed by the aggregation of nanoparticles at the nucleation stage of growth. In the case of CNT growth without an electrical field, the CNTs would grow in a curly fashion. If the density of small-sized catalytic islands on the substrate is low, CNTs would grow in random orientations or in a less-aligned manner, resulting in a low growth rate of the CNT film. Figure 14(a) shows a cross-sectional SEM image of the DWNT film grown from Co nanoparticles deposited by 250 shots using pulsed arc plasma (cumulative Co particle number density of $2 \times 10^{13} \text{ cm}^{-2}$ on the surface). These were nearly optimum conditions for the dense nucleation of DWNTs. As shown in Fig. 14(a), nanotube bundles grew almost straight up due to the high density of DWNTs, corresponding to the high growth rate of 600 nm/s for a growth time of 5 min. On the other hand, for growth on a

substrate with low-density Co nanoparticles, the growth rate of the DWNT film decreased. Figure 14(b) shows a cross-sectional SEM image of DWNT film grown from Co nanoparticles deposited by 50 shots, corresponding to the Co particle number density of $4 \times 10^{12} \text{ cm}^{-2}$ on the surface. As shown in Fig. 14(b), the DWNTs grew in a curly fashion because individual nanotubes had more free space to grow, resulting in the formation of wavy tubes leading to a reduction of the CNT film growth rate (135 nm/s for growth lasting 5 min) compared to Fig. 14(a).

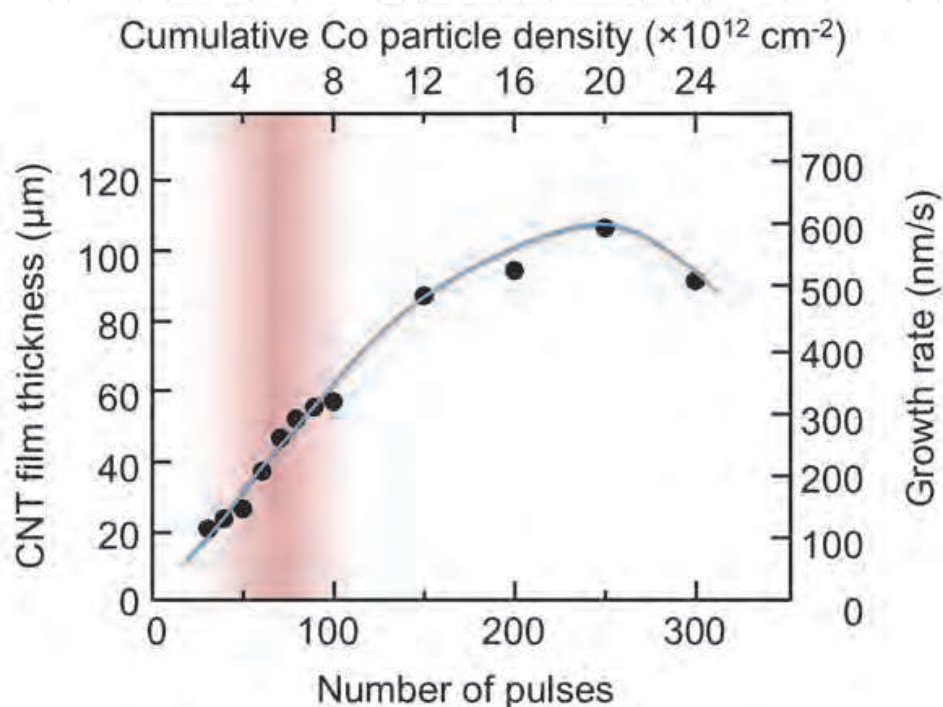


Fig. 13. Variation of thickness of DWNT films grown for 3 min and corresponding growth rate as a function of number of pulses of the pulsed arc discharge plasma for the preparation of Co nanoparticles (or estimated cumulative Co nanoparticle number density on the TiN buffer layer). Masked area corresponds to the condition where self-assembled cone-shaped tips composed of CNT bundles were formed; pulsed arc plasma with 50–100 pulses (see section 4.5).

4.3 SWNT growth from Co and Ti nanoparticles without buffer layer

In the previous section, rapid growth of aligned DWNT films were demonstrated, where catalytic Co nanoparticles were prepared by pulsed arc deposition on a TiN buffer layer. By forming metal nanoparticles employing the pulsed arc discharge with a metal electrode, the density of catalyst nanoparticles with a relatively uniform size can be easily controlled on the substrate. As shown in Fig. 12, by decreasing the number of arc discharge pulses from 250 down to 50 shots, the average diameter of DWNTs decreased from 4.5 nm down to 3.5 nm. However, aligned SWNTs were not grown even at a low density of Co nanoparticles less than 50 pulses, probably because closely adjacent or overlapped Co nanoparticles would easily join together on the TiN surface to increase the size of the nanoislands during the substrate heating, resulting in the formation of less-aligned, low-density DWNTs or randomly oriented, sparse SWNTs after all.

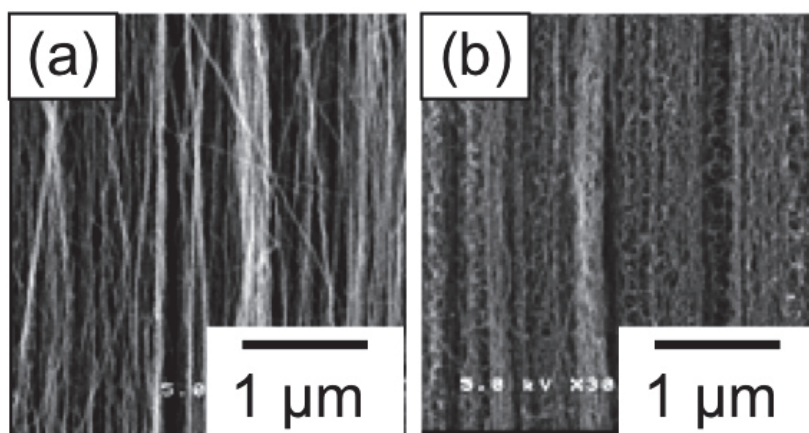


Fig. 14. Cross-sectional SEM images of CNT films grown from Co nanoparticles prepared on TiN buffer layer using pulsed arc plasma with (a) 250 pulses and (b) 50 pulses. (Hiramatsu et al., 2005b) - reproduced with permission from Institute of Pure and Applied Physics

In order to grow SWNT film on a Si substrate, a mixture of Co and Ti nanoparticles was prepared on the Si substrate using pulsed arc plasma deposition with a Co-Ti composite electrode, without a buffer layer. Figure 15 shows a schematic diagram of catalyst preparation for growing CNTs with smaller diameters. Ti is highly reactive with Si to form a silicide, as compared with Co (Murarka, 1983). Accordingly, it is expected that the formation of a Ti-silicide would precede the formation of a Co-silicide, when Ti is mixed with Co. Therefore, Ti prevents the formation of Co-silicide to a certain extent in the substrate heating process, and enables the size of the Co catalyst nanoparticles to be maintained at approximately 1–2 nm. As a result, the fabrication of films composed of vertically aligned SWNTs on Si substrates was attained using microwave plasma-enhanced CVD (Hiramatsu et al., 2007a). Moreover, the controlled preparation of catalyst nanoparticles on the Si substrate was performed by pulsed arc plasma deposition with the alternate use of Co and Ti electrodes. This technique has potential for controlling the size of catalyst nanoislands on the substrate, resulting in the controlled growth of aligned CNTs with single to three walls. By changing the number of cumulative Co nanoparticles, the fabrications of SWNT and DWNT films can be controlled (Hiramatsu et al., 2007b).

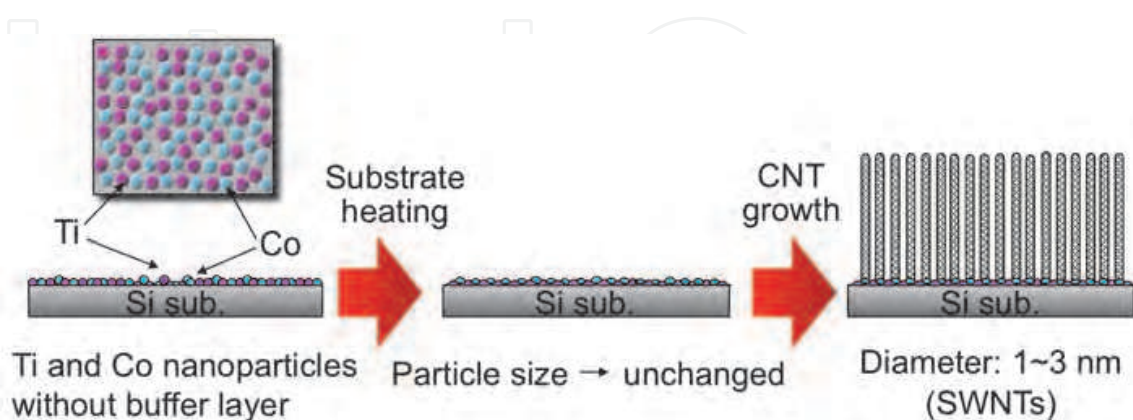


Fig. 15. Schematic of catalyst preparation for growing CNTs with small diameters (SWNTs)

In the case using sintered Ti-Co composite target electrode, the pulsed arc discharge yields a mixture of Co and Ti nanoparticles simultaneously. The sintered Ti-Co composite electrode

is commercially available from ULVAC, Inc., and the Co and Ti contents in the composite are 55.2 and 44.8 wt.%, respectively. The pulsed arc discharge was operated with sintered Ti-Co composite electrode at a pressure of 10^{-4} Torr at room temperature. Three types of Co-catalyzed Si substrates (types A, B and C) without buffer layer were prepared by setting the number of pulsed arc discharges with the Ti-Co composite electrode at 50, 100 and 250 shots, respectively. Ti nanoparticles mixed with the Co nanoparticles prevent the formation of Co-silicide during the substrate heating process, and enables the size of the Co catalytic nanoparticles to be maintained at approximately 1–2 nm.

CNT films were grown using microwave plasma-enhanced CVD with a 2.45 GHz, 1.5 kW microwave generator. A mixture of CH_4 and H_2 was used as the source gas. The flow rates of CH_4 and H_2 were 50 and 70 sccm, respectively. The microwave power and total pressure were maintained at 900 W and 70 Torr, respectively. The growth experiments were carried out for 5 min at a substrate temperature of 700 °C. SEM and TEM were used to evaluate the morphology of the grown CNTs. Raman spectra for the CNTs were obtained using the 514.5 nm line of Ar laser and the 632.8 nm line of He-Ne laser.

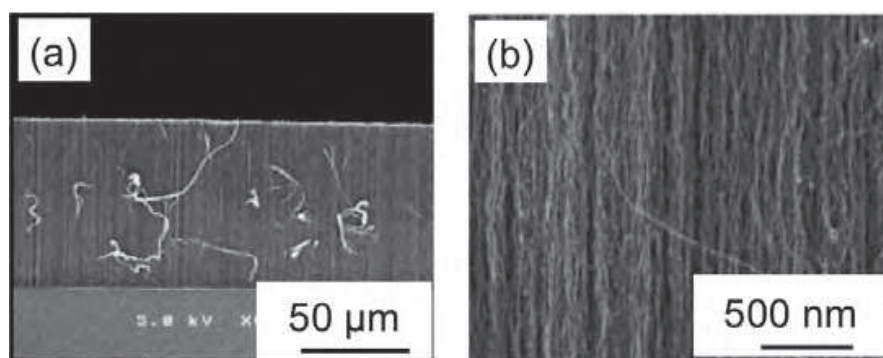


Fig. 16. SEM micrographs of a CNT film grown on a Co-catalyzed Si substrate (type A). The catalytic nanoparticles were prepared by pulsed arc discharge using a sintered Ti-Co composite electrode with 50 pulses. (a) Cross-sectional SEM image of the dense CNT film. (b) Close-up image of the cleaved CNT film showing aligned growth of the nanotubes. (Hiramatsu et al., 2007a) - reproduced with permission from Elsevier

Figure 16(a) shows a typical cross-sectional SEM image of a cleaved CNT film grown for 5 min on a type A substrate. The catalytic nanoparticles were prepared using pulsed arc discharges employing the sintered Ti-Co composite electrode with 50 pulses. A dense and vertically aligned CNT film was observed to grow on the Co-catalyzed Si substrate. Figure 16(b) shows a close-up SEM image of the cleaved CNT film. The morphology in Fig. 16(b) shows that the CNT bundles were not perfectly straight. In this case, the growth rate of the CNT film was approximately 190 nm/s.

Figure 17(a) shows the Raman spectrum at the low frequency band ($100\text{--}400\text{ cm}^{-1}$) for the CNT sample on the type A substrate measured using the 632.8 nm line. The radial breathing mode (RBM) peaks are clearly observed at 188, 260, 282 and 295 cm^{-1} , confirming the existence of SWNTs. Figure 17(b) shows the Raman spectrum at the low frequency band for the same CNT sample measured using the 514.5 nm line. In this case, the RBM peaks are clearly observed at 193, 211, 224, 235, 267 and 290 cm^{-1} . The diameter distribution calculated from the frequency of the RBM peaks for the SWNT bundles is in the range between 0.8 and 1.3 nm.

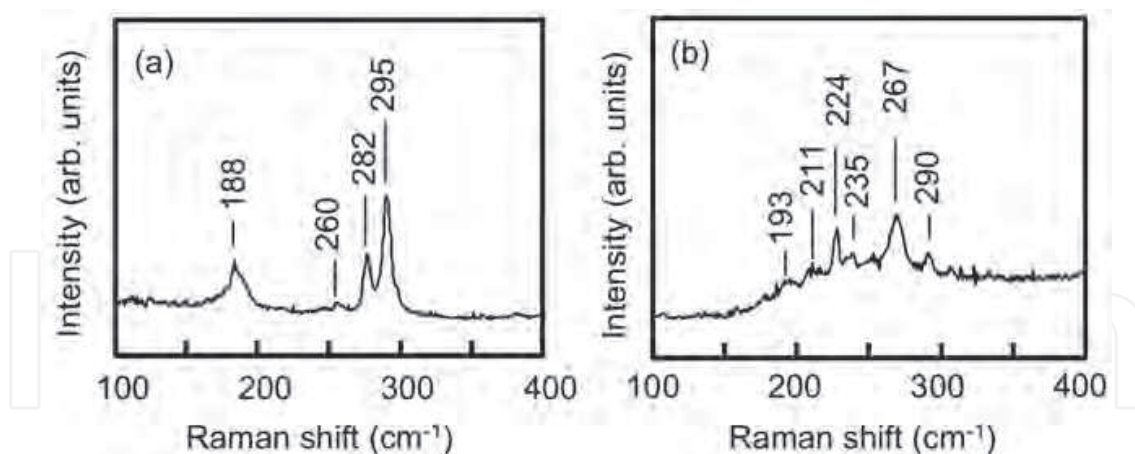


Fig. 17. Raman spectra at the low frequency band (100–400 cm^{-1}) for the CNT sample grown on the type 'A' substrate. The Raman spectra (a) and (b) were obtained using the 632.8 nm line of He-Ne laser and the 514.5 nm line of Ar laser, respectively. (Hiramatsu et al., 2007a) - reproduced with permission from Elsevier

In order to evaluate the morphology and diameter distribution of the CNTs, TEM images were taken for the same CNT sample used for the measurement of Raman spectra shown in Figs. 17(a) and 17(b). A distribution histogram of nanotube outer diameters is shown in Fig. 18, and the typical TEM image of the CNTs is shown in the inset in Fig. 18. The TEM specimen was prepared by scraping from the substrate and ultrasonicing in methanol. The inset TEM image in Fig. 18 reveals that most CNTs are SWNTs free of metal particles. The diameters of the SWNTs were measured and the average diameter of the CNTs was determined to be approximately 1 nm, in agreement with the value calculated from the RBM peaks of the Raman spectra in Figs. 17(a) and 17(b). The distribution histogram of nanotube outer diameters shows that the diameters of most CNTs were in the range from 0.5 to 3 nm. The SWNT and DWNT fractions were estimated to be 80 and 20%, respectively.

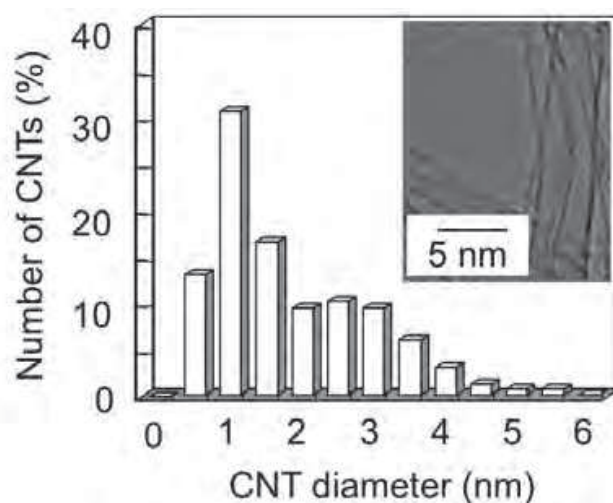


Fig. 18. Distribution histogram of nanotube outer diameters deduced from TEM observations. The CNTs were grown on the type A substrate. The catalytic nanoparticles were prepared by pulsed arc discharges with the sintered Ti-Co composite electrode with 50 pulses. The inset shows a magnified TEM image of typical CNTs. (Hiramatsu et al., 2007a) - reproduced with permission from Elsevier

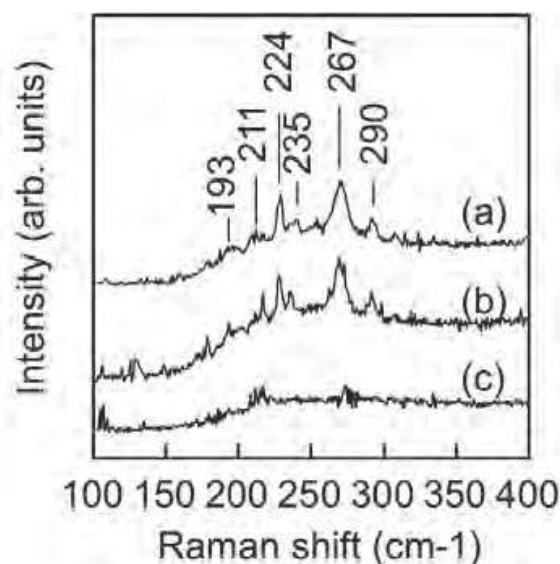


Fig. 19. Raman spectra at the low frequency band (100–400 cm^{-1}), measured using the 514.5 nm line of Ar laser, for CNTs grown on Si substrates with different densities of cumulative nanoparticles. Raman spectra (a)–(c) were obtained for CNT films grown on Co-catalyzed Si substrates, types A, B and C, respectively. (Hiramatsu et al., 2007a) - reproduced with permission from Elsevier

CNTs were grown on Si substrates with different densities of cumulative nanoparticles, and the Raman spectra for the CNTs were obtained using the 514.5 nm line of an Ar laser. In Fig. 19, the Raman spectra (a)–(c) in the low frequency band were obtained for CNT films grown on Co-catalyzed Si substrates, types A, B and C, respectively. As mentioned before, in the Raman spectrum (a) for the CNTs grown on the type A substrate, the RBM peaks are clearly observed at 188, 217, 260, 279 and 293 cm^{-1} , confirming the existence of SWNTs. In the case of the type B substrate, where the cumulative nanoparticle density was twice that on the type A substrate, the RBM peaks are also clearly observed in the Raman spectrum (b). The Raman spectrum (b) is almost identical to the Raman spectrum (a). On the other hand, the growth rate of the CNT film using the type B substrate was approximately 350 nm/s, which is almost twice that of the type A substrate. When using a substrate with low-density catalytic nanoparticles (type A substrate), the CNT bundles had more space to grow and thereby grew in a curly fashion, as shown in Fig. 16(b). With increasing cumulative density of catalytic nanoparticles, as in the case using the type B substrate, SWNT film with a high growth rate was attained due to the dense nucleation of CNTs from the doubled density of the catalytic nanoparticles as compared to the case using the type A substrate. In contrast, with further increase in the cumulative catalytic nanoparticle density, the RBM peaks disappeared, as seen in the Raman spectrum (c) for the CNTs grown on the type C substrate, resulting in the growth of MWNTs with two walls or more.

Figures 20(a) and 20(b) show SEM images of the surfaces of the type B and C Co-catalyzed Si substrates respectively, just before the introduction of CH_4 at a substrate temperature of 700 $^{\circ}\text{C}$. In Fig. 20(a), nanoparticles with a size of approximately 2 nm were formed on the type B substrate. On the other hand, nanoparticles with a size of approximately 3–4 nm were observed on the type C substrate, as seen in the SEM image in Fig. 20(b). Pulsed arc plasma deposition with the Co electrode yielded Co nanoparticles of about 1–2 nm in size. At an appropriate density of catalytic nanoparticles, the catalytic nanoparticles deposited by

pulsed arc discharge play an important role as a template for the growth of SWNTs with diameters as small as 1–2 nm. On the other hand, in the case of growth on a substrate with an excess density of cumulative nanoparticles, MWNTs with 2 or 3 walls were primarily grown. In our system, it takes about 10 min to increase the substrate temperature from room temperature to 700 °C. During this period, overlapping or closely adjacent particles can merge, resulting in the formation of catalytic nanoparticles of approximately 3–4 nm in size.

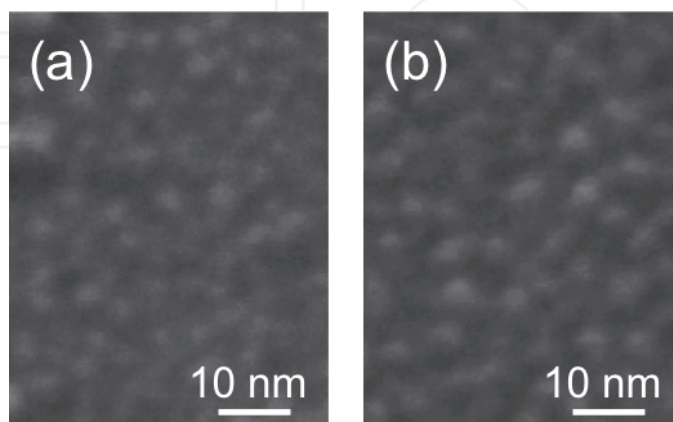


Fig. 20. SEM images of the surface of Co-catalyzed Si substrates: (a) type B and (b) type C, just before introducing CH₄ at a substrate temperature of 700 °C. (Hiramatsu et al., 2007a) - reproduced with permission from Elsevier

Further controlled preparation of catalyst nanoparticles on the Si substrate was performed by pulsed arc plasma deposition with the alternate use of Co and Ti electrodes. This technique has potential for controlling the size of catalyst nanoparticles on the substrate, resulting in the controlled growth of aligned CNTs with single to three walls. By changing the number of cumulative Co nanoparticles, the fabrications of SWNT and DWNT films can be controlled.

In this case, Co and Ti nanoparticles are deposited alternately on the Si substrate without a buffer layer, by pulsed arc discharge with the alternate use of Ti and Co electrodes at a pressure of 10⁻⁴ Torr at room temperature. Ti and Co electrodes were used in turn after every 10 shots of pulsed discharge. The number of cumulative pulsed discharges with the Ti electrode was the same as that with the Co electrode for each substrate prepared for the CNT growth experiment hereafter. The density of Co nanoparticles on the substrate was controlled by varying the number of pulsed discharges with the Co electrode in the range from 50 to 250 shots, resulting in cumulative Co particle densities of 4×10^{12} to 2×10^{13} cm⁻². From the TEM observation, the pulsed arc discharge with the Ti electrode yields Ti nanoparticles as small as the Co nanoparticles. For Co or Ti film deposition by pulsed arc discharge, the deposition rate of the Co film using the Co electrode was almost the same as that of the Ti film using the Ti electrode. Therefore, it would be assumed that the cumulative densities of Ti and Co nanoparticles are almost the same for each substrate prepared.

Figure 21(a) shows a typical cross-sectional SEM image of a cleaved CNT film grown for 5 min on a Co-catalyzed Si substrate with a cumulative Co nanoparticle density of 4×10^{12} cm⁻². A dense and vertically aligned CNT film was grown on the Co-catalyzed Si substrate. Figure 21(b) shows a magnified SEM image of the cleaved CNT film. From the morphology shown in Fig. 21(b), it can be observed that CNT bundles with a diameter of less than 10 nm grew almost vertically, due to the high density of the CNTs. In this case, the growth rate of the SWNT film was approximately 200 nm/s. Figure 21(c) is a typical top-view SEM image

showing the smooth surface of the CNT film. Figure 21(d) shows the TEM image of CNTs, which were scraped away from the substrate and were ultrasonicated in methanol. TEM image shown in Fig. 21(d) reveals that most CNTs are SWNTs without metal particles.

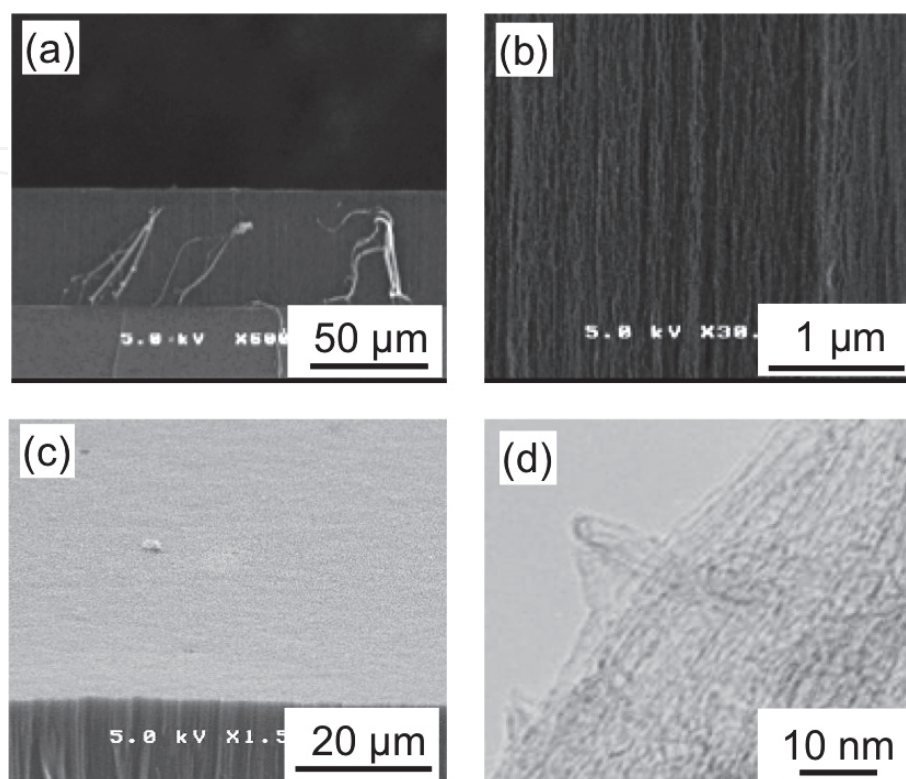


Fig. 21. SEM and TEM micrographs of vertically aligned SWNT film grown for 5 min. (a) Cross-sectional SEM image of cleaved CNT film. (b) Magnified view of the same cleaved CNT film showing aligned growth of nanotubes. (c) SEM image showing the surface of the CNT film. (d) TEM image of CNTs scraped from the substrate. The cumulative Co nanoparticle density was approximately $4 \times 10^{12} \text{ cm}^{-2}$ for the preparation of the Co-catalyzed Si substrate. (Hiramatsu et al., 2007b) - reproduced with permission from Institute of Pure and Applied Physics

Raman spectra of the CNT samples were measured using the 632.8 nm line of He-Ne laser. In Fig. 22, the Raman spectra (a)–(c) at a low frequency band ($100\text{--}400 \text{ cm}^{-1}$) were obtained for CNT films grown on Co-catalyzed Si substrates with cumulative Co nanoparticle densities of 4×10^{12} , 1.2×10^{13} , and $2 \times 10^{13} \text{ cm}^{-2}$, respectively. In the Raman spectrum shown in Fig. 22(a), for CNTs grown on a Co-catalyzed Si substrate with a cumulative Co nanoparticle density of $4 \times 10^{12} \text{ cm}^{-2}$, the radial breathing mode (RBM) peaks are clearly observed at 188, 217, 260, 279, and 293 cm^{-1} confirming the existence of SWNTs. The diameter distribution calculated from the frequency of the RBM peaks for SWNT bundles is in the range between 0.8 and 1.3 nm. With an increasing cumulative density of the Co nanoparticles on the Si substrate, the intensities of the RBM peaks in the Raman spectrum (b) decreased, suggesting that the CNTs grown in this case were a mixture of SWNTs and MWNTs with two or three walls. With further increase in the number of cumulative Co nanoparticles up to $2 \times 10^{13} \text{ cm}^{-2}$, the RBM peaks disappeared as observed in the Raman spectrum (c), resulting in the growth of MWNTs with more than two walls.

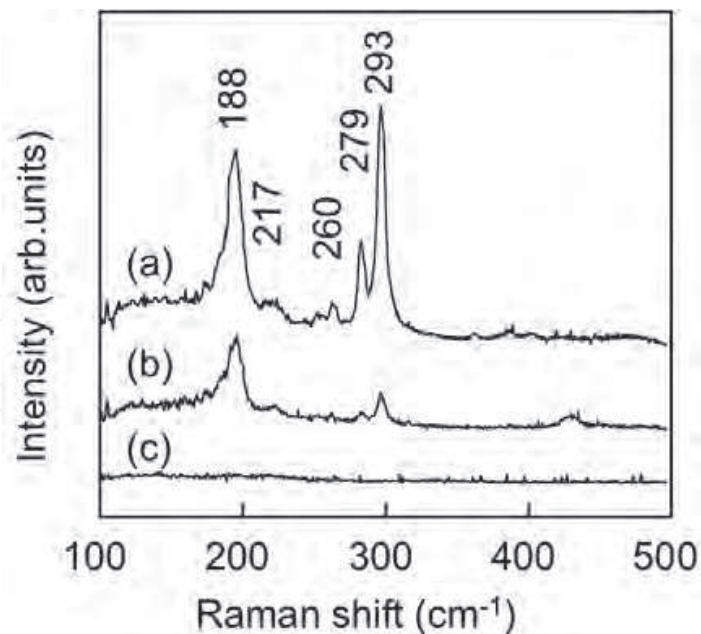


Fig. 22. Raman spectra at low frequency band (100–400 cm^{-1}) for CNT samples, measured using 632.8 nm line of He-Ne laser. Raman spectra (a)–(c) were obtained for CNT films grown on Co-catalyzed Si substrates with cumulative Co nanoparticle densities of 4×10^{12} , 1.2×10^{13} , and $2 \times 10^{13} \text{ cm}^{-2}$, respectively. (Hiramatsu et al., 2007b) - reproduced with permission from Institute of Pure and Applied Physics

Figures 23(a)–23(c) show the TEM images of CNTs grown on Co-catalyzed Si substrates with cumulative Co nanoparticle densities of 4×10^{12} , 1.2×10^{13} , and $2 \times 10^{13} \text{ cm}^{-2}$, respectively. Figures 23(d)–23(f) show the distribution histograms of the nanotube outer diameters, corresponding to the CNTs shown in Figs. 23(a)–23(c), respectively. For CNTs grown on a Co-catalyzed Si substrate, with a cumulative Co nanoparticle density of $4 \times 10^{12} \text{ cm}^{-2}$, the TEM image shown in Fig. 23(a) reveals that most CNTs are SWNTs without metal particles. The diameters of SWNTs were measured and found to be in the range of 1 to 2 nm, in agreement with that calculated from the RBM peaks of the Raman spectrum shown in Fig. 22(a). Note that after an ultrasonic treatment for the preparation of TEM specimens, most SWNTs were still in bundles, due to the van der Waals attraction. The distribution histogram of nanotube outer diameters shown in Fig. 23(d) shows that the CNTs had small average diameters and a narrow diameter distribution centered at approximately 1.5 nm. The percentages of SWNTs and DWNTs were estimated to be 85 and 15%, respectively. On the other hand, for CNTs grown on a Co-catalyzed Si substrate with a cumulative Co nanoparticle density of $1.2 \times 10^{13} \text{ cm}^{-2}$, majority of the CNTs were DWNTs with an average outer diameter of approximately 4 nm, as observed in the TEM image shown in Fig. 23(b). From the distribution histogram of the nanotube outer diameters shown in Fig. 23(e), the CNTs were a mixture of SWNTs, DWNTs, and MWNTs with three walls. The percentage of DWNTs was estimated to be 60%. With further increase in the cumulative Co nanoparticle density up to $2 \times 10^{13} \text{ cm}^{-2}$, as shown in Figs. 23(c) and 23(f), the distribution of the grown CNTs changed to a mixture of DWNTs and MWNTs with three or four walls. The diameters of most CNTs were measured and were in the range of 5 to 7 nm.

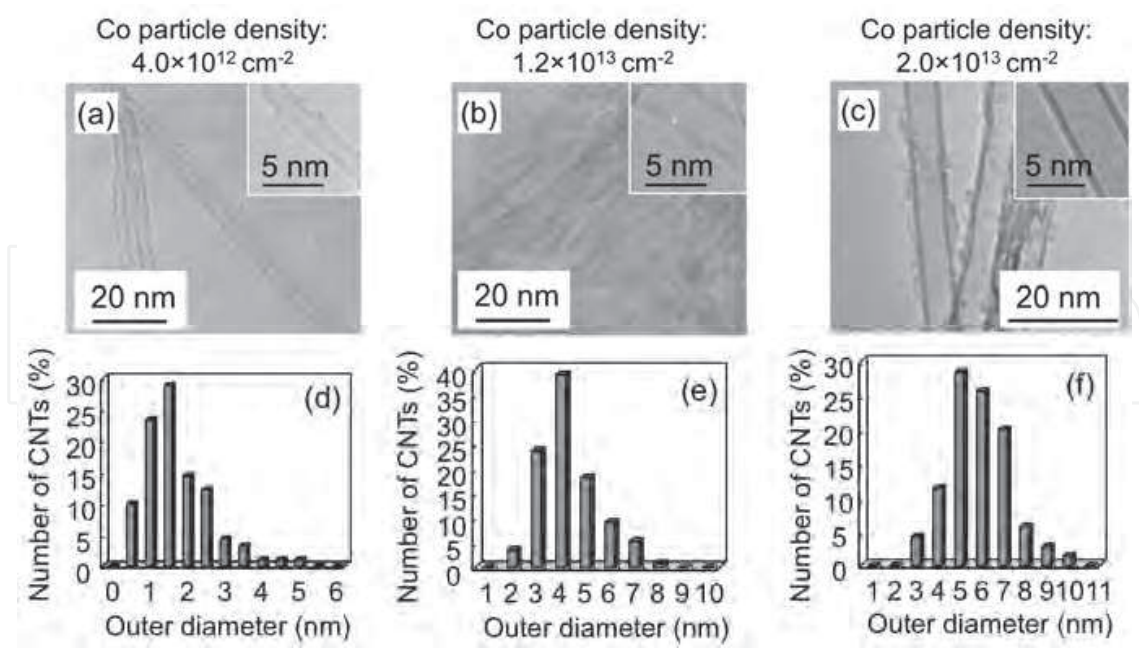


Fig. 23. (a)–(c) TEM images of CNTs grown on Co-catalyzed Si substrates with cumulative Co nanoparticle densities of 4×10^{12} , 1.2×10^{13} , and $2 \times 10^{13} \text{ cm}^{-2}$, respectively. (d)–(f) Corresponding distribution histograms of nanotube outer diameters deduced from TEM observations in (a)–(c), respectively. (Hiramatsu et al., 2007b) - reproduced with permission from Institute of Pure and Applied Physics

4.4 Area-selective growth of aligned CNTs

Well-defined, organized CNT structures were thus fabricated. The catalytic nanoparticles were patterned using a lift-off method, and aligned SWNTs were selectively grown on the patterned catalytic particles, which resulted in the fabrication of organized microstructures of aligned SWNTs and DWNTs.

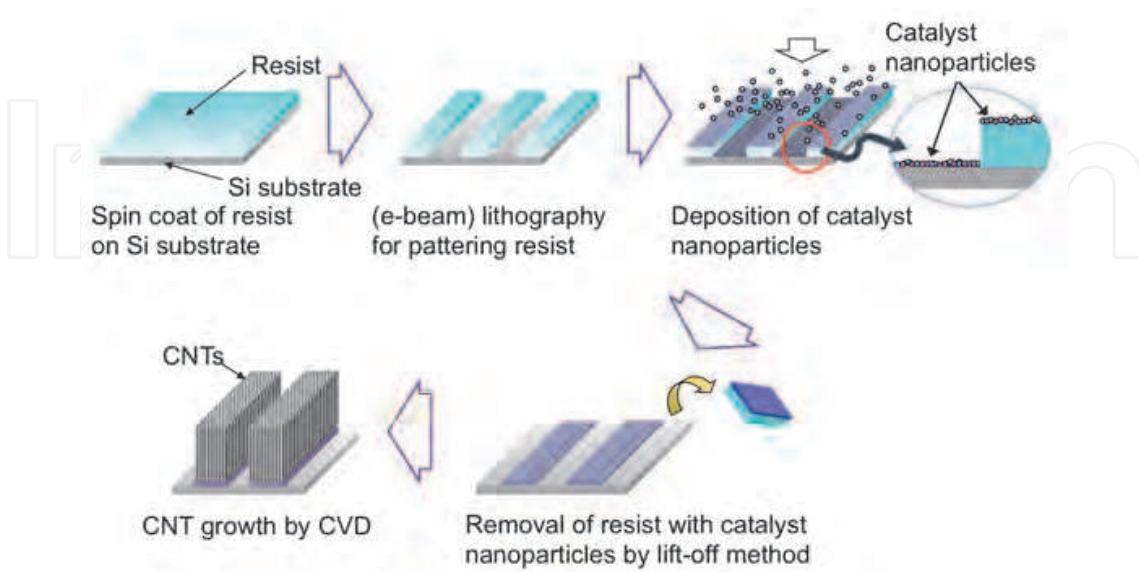


Fig. 24. Schematic diagram for patterning catalyst nanoparticles by lift-off method and area-selective growth of aligned CNTs.

Figure 24 shows a schematic procedure for patterning catalyst nanoparticles by a lift-off method and area-selective growth of aligned CNTs. "Lift-off" is a simple, easy method for patterning films that are deposited. In this case, catalyst nanoparticles are deposited area-selectively on a Si substrate. First, a pattern is defined on the Si substrate using photoresist. By using the pulsed arc discharge, a mixture of Co and Ti nanoparticles are deposited on the photoresist as well as the areas in which the photoresist has been cleared. Then, the photoresist is removed with solvent, taking the metal nanoparticles with it, and leaving only the nanoparticles deposited directly on the substrate. As a result, CNTs are grown area-selectively on the patterned catalyst nanoparticles.

Dense and aligned SWNTs with controlled microstructures were grown from the patterned catalytic nanoparticles, as demonstrated in Figs. 25(a)–25(f). Figure 25(a) shows a SEM top-view image of wavy lines with 1 μm width of vertical SWNTs grown on striped patterns of catalytic nanoparticles, showing area-selective growth of the vertically aligned SWNT film. Furthermore, SWNT pillars with a high aspect ratio were fabricated successfully. Figure 25(b) shows a SEM image of arrays of SWNT cylindrical pillars 100 μm long and 800 nm in diameter, forming a brush structure. A close-up view of the SWNT cylindrical pillars 10 μm long and 800 nm in diameter is shown in Fig. 25(c). Figures 25(d)–25(f) show another examples of organized SWNT microstructures: logos of Nano Factory and Meijo University written in kanji (Chinese character).

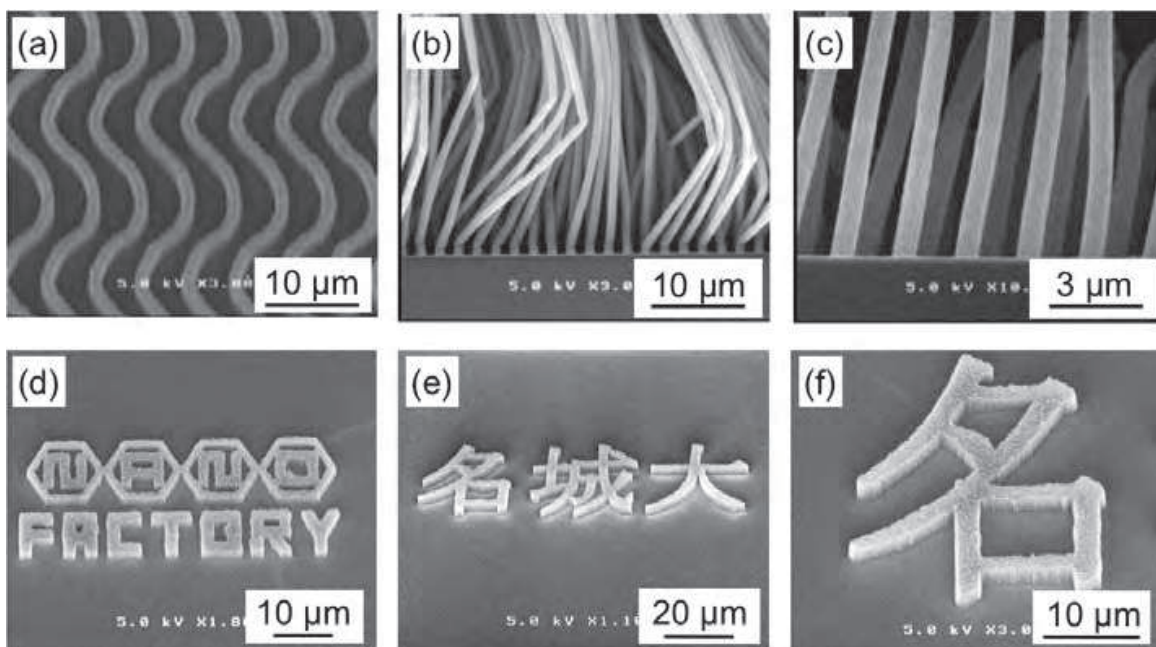


Fig. 25. SEM images of organized SWNT structures grown on patterned catalytic nanoparticles: (a) Wavy lines with 1 μm width, (b) side view of arrays of SWNT cylindrical pillars 100 μm long and 800 nm in diameter, (c) close-up view of SWNT cylindrical pillars 10 μm long and 800 nm in diameter, (d) logo of Nano Factory, (e) logo of Meijo University written in kanji (Chinese character), and (f) close-up view of kanji composed of aligned SWNTs. (Hiramatsu et al., 2007a) - reproduced with permission from Elsevier

CNTs are expected to be used as vertical wiring materials for future large-scale integrated circuits (LSI) interconnects (Horibe et al., 2005; Robertson et al., 2009; Nihei et al., 2010). For this purpose, aligned SWNT pillars were selectively grown on the bottom of the via-holes

created in the thick SiO₂ film. Figure 26 shows a schematic procedure for growing vertically aligned SWNTs in the via-holes. The 800-nm-thick SiO₂ film was etched to form holes with 800 nm in diameter by conventional lithography and dry etching. Before removing the photoresist, catalyst nanoparticles were prepared on the photoresist as well as at the bottom of the holes by pulsed arc plasma deposition with the alternate use of Co and Ti electrodes or the sintered Ti-Co composite electrode. After removing the photoresist, catalyst nanoparticles remained only at the bottom of the holes. Finally, aligned CNTs are grown area-selectively from the catalyst nanoparticles deposited on the bottom of the via-holes.

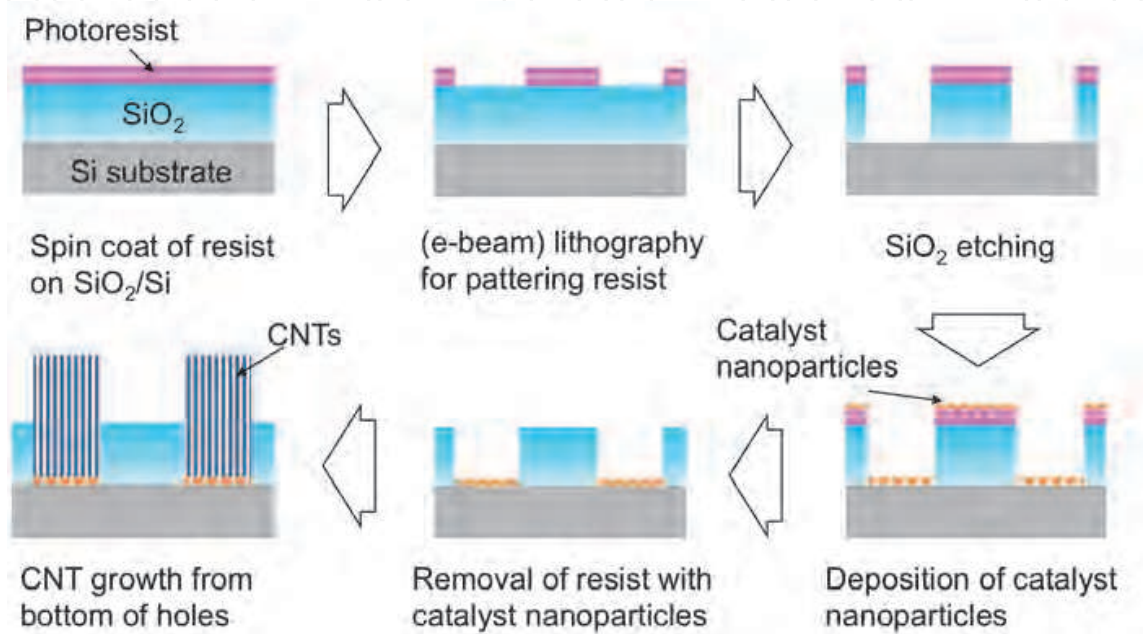


Fig. 26. Schematic diagram for growing vertically aligned SWNTs in the via-holes.

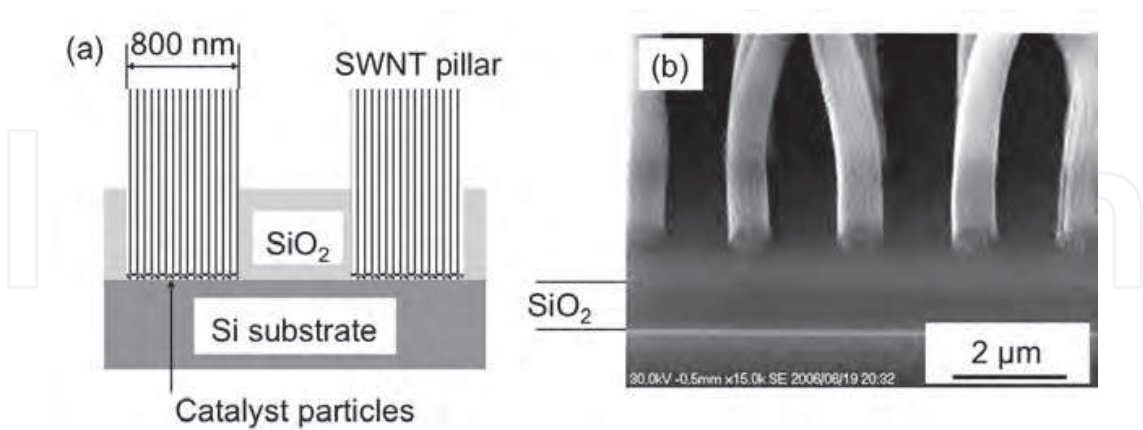


Fig. 27. (a) Schematic of vertical SWNTs embedded in holes drilled in SiO₂ film on Si substrate. (b) SEM image of SWNT cylindrical pillars of 800 nm in diameter, grown from the bottom of holes drilled in SiO₂ film. (Hiramatsu et al., 2007b) - reproduced with permission from Institute of Pure and Applied Physics

Figure 27(a) shows a schematic of vertically aligned SWNTs embedded in holes drilled in a SiO₂ film on the Si substrate. Figure 27(b) shows a SEM image of SWNT cylindrical pillars of

800 nm in diameter, grown from the bottom of the holes drilled in the SiO₂ film. In the case of the actual interconnects, planarization process using the chemical mechanical polishing (CMP) should be conducted after the CNT growth. Furthermore, TiN or Ti as the contact layer would exist at the bottom of the via-holes. Therefore, the technique for growing aligned DWNTs shown in Section 4.2 would be suitable for the practical application to the vertical wiring for the future LSI interconnects.

4.5 Growth of self-assembled cone-shaped tip arrays for emitter application

When the density of aligned CNTs is high, it is considered that such conditions are effective in the vertical wiring of next-generation integrated circuits. However, from the viewpoint of applications to field electron emission devices, although a threshold electric field that can be expected in the case of DWNTs is as low as that in the case of SWNTs, too high density of the CNTs has an adverse effect on electron emission devices because it reduces the electric fields applied to each nanotube. For this purpose, it is necessary to isolate DWNTs or to create a new shape for bundles. If the density of small-sized catalytic particles on the substrate is significantly low, CNTs would grow in random orientations or in a less-aligned manner, and isolated DWNTs could not be grown.

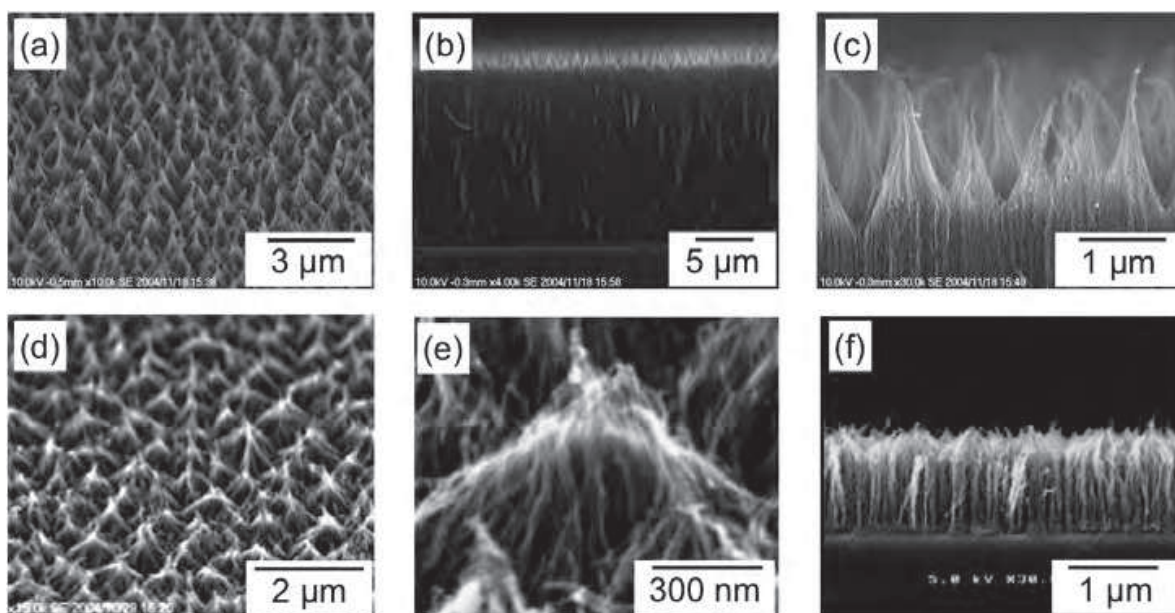


Fig. 28. SEM micrographs of DWNT films with self-assembled conical tip arrays grown on a Co-catalyzed Si substrate with a TiN buffer layer. The Co particles were prepared using pulsed arc plasma deposition with 50 pulses. (a) Tilted-view SEM image of DWNT film grown for 3 min, (b) cross-sectional SEM image of vertically aligned DWNT film, and (c) close-up image of self-assembled conical tips. (d) Tilted-view image, (e) close-up image, and (f) cross-sectional SEM image of DWNT film grown for 5 sec. (Hori et al., 2006)

The density of Co nanoparticles was reduced to some extent in comparison with the case for the growth of dense DWNTs shown in Fig. 9. When the number of shots of pulsed arc plasma was adjusted to approximately 50, the growth rate of CNT films decreased to approximately 200 nm/s. In this case, however, DWNT films possessing self-assembled cone-shaped tips at the top were formed as shown in the SEM photographs of Figs. 28(a)–28(c). A tilted-view SEM image of aligned DWNT film grown on Co-catalyzed Si substrate

with TiN buffer layer is shown in Fig. 28(a). Co particles were prepared using pulsed arc plasma deposition with 50 pulses, corresponding to the cumulative particle number density of approximately $4 \times 10^{12} \text{ cm}^{-2}$ on the surface. As shown in Fig. 28(a), self-assembled conical tips were fabricated on the top of aligned DWNT film. Cross-sectional SEM images of vertically aligned DWNT film with self-assembled conical tip arrays are shown in Figs. 28(b) and 28(c). The height of conical parts was approximately $1 \mu\text{m}$, and their distance was approximately 500 nm , as shown in Fig. 28(c). It was found that individual CNTs were not straight, but grown almost vertically, via a self-support mechanism, due to the high density of the CNTs. Figures 28(d)–28(f) show SEM images of DWNT film with conical tips grown for 5 sec. At this moment, the height of conical parts was less than 500 nm and their shape was not clearly defined.

In the case of the growth of single-walled or double-walled thin nanotubes with a certain space, tubes can swing relatively freely in an early stage of the growth. By setting space without causing the falling of the tubes, loosely-packed bundles are easily formed because of van der Waals force to make up cone-shaped tips at the top. It is noted that the self-assembled cone-shaped tips composed of CNT bundles were formed from Co nanoparticles with cumulative particle densities of $4\text{--}8 \times 10^{12} \text{ cm}^{-2}$. In Fig. 13, masked area corresponds to the condition where self-assembled cone-shaped tips were formed. The surface morphology of cone-shaped tip arrays does not depend on the growth period of nanotubes, while the CNT film thickness increased linearly with the growth period up to 10 min. In other words, the surface shape of films in the case of 30 seconds growth is the same as that in the case of 10 minutes growth, and the growth process of carbon nanotubes in this experiment is the evidence of base growth.

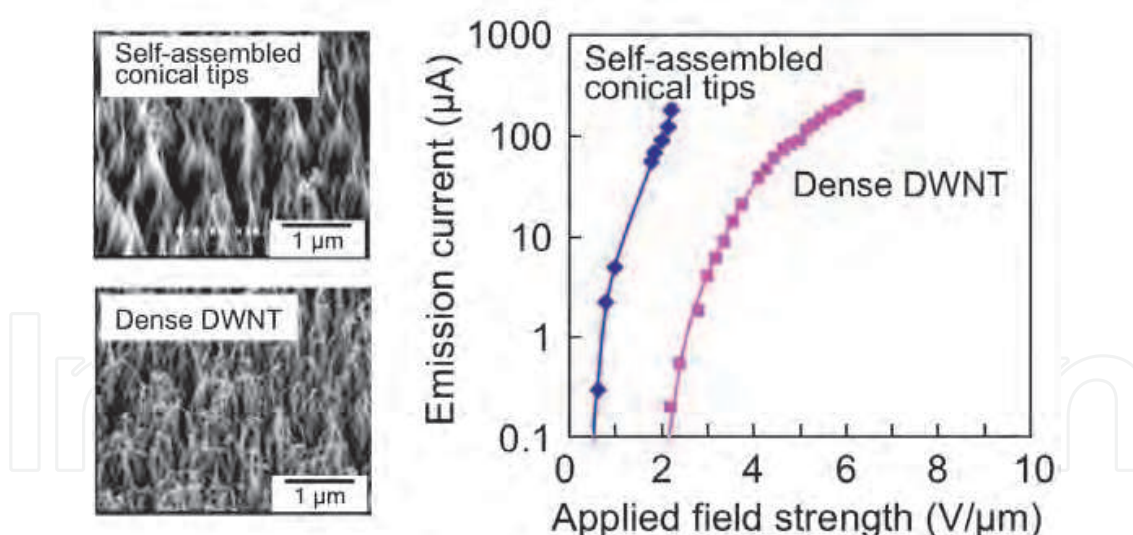


Fig. 29. Field emission characteristics of DWNT film with self-assembled conical tips and dense DWNT film.

Regarding DWNT films with self-assembled cone-shaped tips at the top, the field electron emission characteristics were measured. The field emission properties of as-grown DWNT film with self-assembled conical tips and dense DWNT film were investigated in a homemade parallel-plate diode device with the CNT film as a cathode and a stainless steel rod (1.5 mm in diameter) as an anode in a vacuum chamber (10^{-6} Torr). Negative voltages were applied to the CNT film and corresponding emission currents were recorded. The

distance between anode and cathode (CNT film) was kept at 500 μm . The electric field is expressed as the applied voltage divided by the anode to sample distance. The electron field emission properties of DWNT film with self-assembled conical tips and dense DWNT film are shown in Fig. 29. As a result of the measurement, the onset electric field for the electron field emission was below 1 V/ μm for the DWNT film with self-assembled conical tips. The above-mentioned "Spindt-type" CNT bundles are thought to be suitable for the electron field emission application.

5. Conclusion

We have demonstrated the fabrication of films composed of vertically aligned, SWNTs and DWNTs on Si substrates using microwave plasma-enhanced chemical vapor deposition. As the first step of this study, Co nanoparticles were formed on the substrate using pulsed arc plasma deposition. The pulsed arc discharge with a Co electrode yielded Co nanoparticles approximately 1–2 nm in size on the substrate. A TiN thin film was used as a buffer layer in order to prevent the formation of Co silicide. As a result, a dense, vertically aligned DWNT film was grown rapidly on the Co-catalyzed Si substrate. The CNTs grew at an extremely high rate of 600 nm/s. By forming metal nanoparticles employing the pulsed arc discharge with a metal electrode, the density of catalyst nanoparticles with a relatively uniform size can be easily controlled on the substrate. However, closely adjacent or over-lapped Co nanoparticles would easily join together on the TiN surface to increase the size of the particles during the substrate heating, resulting in the growth of DWNTs.

In order to grow SWNT film on a Si substrate, catalytic nanoparticles were formed on Si substrates using pulsed arc plasma deposition with a Co–Ti composite electrode, without buffer layer. Ti nanoparticles mixed with the Co nanoparticles prevents the formation of Co silicide during the substrate heating process, and enables the size of the Co catalytic nanoparticles to be maintained at approximately 1–2 nm. As a result, the fabrication of films composed of vertically aligned SWNTs on Si substrates was attained. Moreover, the controlled preparation of catalyst nanoparticles on the Si substrate was performed by pulsed arc plasma deposition with the alternate use of Co and Ti electrodes. This technique has potential for controlling the size of catalyst nanoparticles on the substrate, resulting in the controlled growth of aligned carbon nanotubes with single to three walls. By changing the number of cumulative Co nanoparticles, the fabrications of SWNT and DWNT films can be controlled. Furthermore, the catalytic nanoparticles were patterned using a lift-off method, and SWNTs and DWNTs were selectively grown on the patterned catalytic particles, which resulted in the fabrication of organized microstructures of aligned CNTs.

6. References

- Agawa, Y.; Yamaguchi, K.; Hara, Y.; Amano, S.; Horiuchi, T. & Shen, G. (2003). "Formation of a hafnium nitride film by an arc plasma gun". *ULVAC Technical Journal*, Vol.57E (2003) 1
- Bower, C.; Zhou, O. ; Zhu, W.; Werder, D. J. & Jin, S. (2000). "Nucleation and growth of carbon nanotubes by microwave plasma chemical vapor deposition". *Applied Physics Letters*, Vol.77, No.17, pp.2767–2769, DOI:10.1063/1.1319529
- Hiramatsu, M.; Taniguchi, M.; Nagao, H.; Ando, Y. & Hori, M. (2005a). "Fabrication of dense carbon nanotube films using microwave plasma-enhanced chemical vapor

- deposition". *Japanese Journal of Applied Physics*, Vol.44, No.2, pp.1150-1154, DOI: 10.1143/JJAP.44.1150
- Hiramatsu, M.; Nagao, H.; Taniguchi, M.; Amano, H. ;Ando, Y. & Hori, M. (2005b). "High-rate growth of films of dense, aligned double-walled carbon nanotubes using microwave plasma- enhanced chemical vapor deposition". *Japanese Journal of Applied Physics*, Vol.44, No.22, pp.L693-L695, DOI: 10.1143/JJAP.44.L693
- Hiramatsu, M.; Deguchi, T.; Nagao, H. & Hori, M. (2007a). "Area-selective growth of aligned single-walled carbon nanotube films using microwave plasma-enhanced CVD". *Diamond & Related Materials*, Vol.16, No.4-7, pp.1126-1130, DOI: 10.1016/j.diamond.2006.11.070
- Hiramatsu, M.; Deguchi, T.; Nagao, H. & Hori, M. (2007b). "Aligned growth of single-walled and double-walled carbon nanotube films by control of catalyst preparation". *Japanese Journal of Applied Physics*, Vol.46, No.3, pp.L303-L306, DOI: 10.1143/JJAP.46.L303
- Hong, W. K.; Chen, K. H.; Chen, L. C.; Tarntair, F. G.; Chen, K. J.; Lin, J. B. & Cheng, H. C. (2001). "Fabrication and characterization of carbon nanotube triodes". *Japanese Journal of Applied Physics*, Vol.40, No.5a, pp.3468-3473, DOI: 10.1143/JJAP.40.3468
- Hori, M.; Hiramatsu, M. & Kano, H. (2006). "Carbon nanotube aggregate and method for producing same". WO/2006/120780
- Horibe, M.; Nihei, M.; Kondo, D.; Kawabata, A. & Awano, Y. (2005). "Carbon Nanotube Growth Technologies Using Tantalum Barrier Layer for Future VLSIs with Cu/Low-k Interconnect Processes". *Japanese Journal of Applied Physics*, Vol.44, No.7A, pp.5309-5312, DOI: 10.1143/JJAP.44.5309
- Kim, U.; Pcioneck, R.; Aslam, D. M. & Tomanek, D. (2001). "Synthesis of high-density carbon nanotube films by microwave plasma chemical vapor deposition". *Diamond and Related Materials*, Vol.10, No.11, pp.1947-1951, DOI: 10.1016/S0925-9635(01)00384-3
- Lee, S. B.; Teh, A. S.; Teo, K. B.; Chhowalla, K. M.; Hasko, D. G.; Milne, W. I.; Amaratunga, G. A. J. & Ahmed, H. (2003). "Fabrication of carbon nanotube lateral field emitters". *Nanotechnology*, Vol.14, No.2, pp.192-195, DOI: 10.1088/0957-4484/14/2/318
- Murakami, Y.; Chiashi, S.; Miyauchi, Y.; Hu, M.; Ogura, M.; Okubo, T. & Maruyama, S. (2004). "Growth of vertically aligned single-walled carbon nanotube films on quartz substrates and their optical anisotropy". *Chemical Physics Letters*, Vol.385, No.3, pp.298-303, DOI: 10.1016/j.cplett.2003.12.095
- Murarka, S. P. (1983). *Silicide for VLSI Applications*, Academic Press, New York, p. 72.
- Nihei, M.; Kawabata, A.; Sato, M.; Nozue, T.; Hyakushima, T.; Kondo, D.; Ohfuti, M.; Sato, S. & Awano, Y. (2010). "Carbon Nanotube Interconnect Technologies for Future VLSIs". In: *Solid State Circuits Technologies*, Jacobus W. Swart, pp.227-238, InTech, ISBN: 978-953-307-045-2
- Robertson, J.; Zhong, G.; Hofmann, S.; Bayer, B. C.; Esconjauregui, C. S.; Telg, H. & Thomsen, C. (2009). "Use of carbon nanotubes for VLSI interconnects". *Diamond and Related Materials*, Vol.18, No.5-8, pp.957-962, DOI: 10.1016/j.diamond.2009.02.008
- Sugai, T.; Yoshida, H.; Shimada, T.; Okazaki, T.; Bandow, S. & Shinohara, H. (2003). "New Synthesis of High-Quality Double-Walled Carbon Nanotubes by High-Temperature Pulsed Arc Discharge". *Nano Letters*, Vol.3, No.6, pp.769-773, DOI: 10.1021/nl034183+

- Sugai, T.; Okazaki, T.; Yoshida, H. & Shinohara, H. (2004). "Syntheses of single- and double-wall carbon nanotubes by the HTPAD and HFCVD methods". *New Journal of Physics*, Vol.6, No.1, (2004), 21, DOI: 10.1088/1367-2630/6/1/021
- Yamamoto, Y.; Agawa, Y.; Hara, Y.; Amano, S.; Chayahara, A.; Horono, Y. & Fujii, K. (1998). "Development of a coaxial type vacuum arc evaporation source". *Proceedings of 12th International Conference on Ion Implantation Technology*, pp.1148-1150
- Zhong, G.; Iwasaki, T.; Honda, K.; Furukawa, Y.; Ohdomari, I. & Kwarada, H. (2005). "Low temperature synthesis of extremely dense and vertically aligned single-walled carbon nanotubes". *Japanese Journal of Applied Physics*, Vol.44, No.4a, pp.1558-1561, DOI: 10.1143/JJAP.44.1558



Carbon Nanotubes - Synthesis, Characterization, Applications

Edited by Dr. Siva Yellampalli

ISBN 978-953-307-497-9

Hard cover, 514 pages

Publisher InTech

Published online 20, July, 2011

Published in print edition July, 2011

Carbon nanotubes are one of the most intriguing new materials with extraordinary properties being discovered in the last decade. The unique structure of carbon nanotubes provides nanotubes with extraordinary mechanical and electrical properties. The outstanding properties that these materials possess have opened new interesting researches areas in nanoscience and nanotechnology. Although nanotubes are very promising in a wide variety of fields, application of individual nanotubes for large scale production has been limited. The main roadblocks, which hinder its use, are limited understanding of its synthesis and electrical properties which lead to difficulty in structure control, existence of impurities, and poor processability. This book makes an attempt to provide indepth study and analysis of various synthesis methods, processing techniques and characterization of carbon nanotubes that will lead to the increased applications of carbon nanotubes.

How to reference

In order to correctly reference this scholarly work, feel free to copy and paste the following:

Mineo Hiramatsu and Masaru Hori (2011). Aligned Growth of Single-Walled and Double-Walled Carbon Nanotube Films by Control of Catalyst Preparation, Carbon Nanotubes - Synthesis, Characterization, Applications, Dr. Siva Yellampalli (Ed.), ISBN: 978-953-307-497-9, InTech, Available from: <http://www.intechopen.com/books/carbon-nanotubes-synthesis-characterization-applications/aligned-growth-of-single-walled-and-double-walled-carbon-nanotube-films-by-control-of-catalyst-prepa>

INTECH
open science | open minds

InTech Europe

University Campus STeP Ri
Slavka Krautzeka 83/A
51000 Rijeka, Croatia
Phone: +385 (51) 770 447
Fax: +385 (51) 686 166
www.intechopen.com

InTech China

Unit 405, Office Block, Hotel Equatorial Shanghai
No.65, Yan An Road (West), Shanghai, 200040, China
中国上海市延安西路65号上海国际贵都大饭店办公楼405单元
Phone: +86-21-62489820
Fax: +86-21-62489821

© 2011 The Author(s). Licensee IntechOpen. This chapter is distributed under the terms of the [Creative Commons Attribution-NonCommercial-ShareAlike-3.0 License](https://creativecommons.org/licenses/by-nc-sa/3.0/), which permits use, distribution and reproduction for non-commercial purposes, provided the original is properly cited and derivative works building on this content are distributed under the same license.

IntechOpen

IntechOpen